Interface focus

J. R. Soc. Interface (2010) **7**, S321–S330
doi:10.1098/rsif.2010.0039.focus
Published online 31 March 2010

Emergence of a prestressed eukaryotic nucleus during cellular differentiation and development

Aprotim Mazumder[1] and G. V. Shivashankar[1,2,*]

[1]*National Centre for Biological Sciences, Tata Institute of Fundamental Research, GKVK Campus, Bellary Road, Bangalore 560065, India*
[2]*Department of Biological Sciences and Research Center for Excellence in MechanoBiology, National University of Singapore, Science Drive 4, Singapore 117543, Republic of Singapore*

Nuclear shape and size are emerging as mechanistic regulators of genome function. Yet, the coupling between chromatin assembly and various nuclear and cytoplasmic scaffolds is poorly understood. The present work explores the structural organization of a prestressed nucleus in a variety of cellular systems ranging from cells in culture to those in an organism. A combination of laser ablation and cellular perturbations was used to decipher the dynamic nature of the nucleo-cytoplasmic contacts. In primary mouse embryonic fibroblasts, ablation of heterochromatin nodes caused an anisotropic shrinkage of the nucleus. Depolymerization of actin and microtubules, and inhibition of myosin motors, resulted in the differential stresses that these cytoplasmic systems exert on the nucleus. The onset of nuclear prestress was then mapped in two contexts—first, in the differentiation of embryonic stem cells, where signatures of prestress appeared with differentiation; second, at an organism level, where nuclear or cytoplasmic laser ablations of cells in the early *Drosophila* embryo induced a collapse of the nucleus only after cellularization. We thus show that the interplay of physical connections bridging the nucleus with the cytoplasm governs the size and shape of a prestressed eukaryotic nucleus.

Keywords: cell nucleus; cytoskeleton; prestress; differentiation; development

1. INTRODUCTION

Nuclear shape and size are emerging as potential regulators of genome function, yet its mechanistic basis is poorly understood (Thomas *et al.* 2002; Lanctot *et al.* 2007; Misteli 2007). An inspection of shapes reveals disc-shaped and elliptical nuclei in several cell types (Schermelleh *et al.* 2008). This implies that the cytoskeleton applies forces to modulate nuclear shape and size, possibly through contacts spanning the nuclear envelope. Recently, a number of links have been delineated between the nuclear envelope and the cytoplasmic filaments (Padmakumar *et al.* 2005; Zhang *et al.* 2005; Crisp *et al.* 2006; Haque *et al.* 2006; Tzur *et al.* 2006; Roux *et al.* 2009; Wang *et al.* 2009). The SUN (Sad 1p, Unc-84) domain proteins on the inner nuclear envelope connect to the KASH (Klarsicht, ANC-1, Syne Homology) domain proteins (like the nesprins) on the outer nuclear envelope, and thus span the approximately 60 nm lumenal space between the two bilayers of the nuclear envelope. The SUN domain proteins in turn interact with the nuclear components such as the chromatin and lamin, while the KASH domain proteins interact with the cytoskeleton (Padmakumar *et al.* 2005; Zhang *et al.* 2005; Crisp *et al.* 2006; Haque *et al.* 2006; Tzur *et al.* 2006; Kracklauer *et al.* 2007; Wang *et al.* 2009). A specialized nuclear-anchoring structure for cytoskeletal filaments, known as the LINC (linker of nucleoskeleton and cytoskeleton) complex, that contains nesprins, sun and lamin proteins has recently been identified (Padmakumar *et al.* 2005; Crisp *et al.* 2006; Haque *et al.* 2006). Concomitant with these discoveries, new insights have been gained into the mechanistic maintenance of the cell nucleus (Lee *et al.* 2007; Stewart *et al.* 2007; Dahl *et al.* 2008; Hale *et al.* 2008; Roux *et al.* 2009). The nuclear lamin proteins are expressed at distinct stages during differentiation (Riemer *et al.* 1995; Constantinescu *et al.* 2006), and are thought to differentially regulate nuclear mechanics (Lammerding *et al.* 2006; Houben *et al.* 2007). Lamin B1 has been shown to be central for the proper development of a mouse embryo (Vergnes *et al.* 2004). Molecules associated with the maintenance of nuclear shape have also been shown to regulate *Drosophila* development (Brandt *et al.* 2006; Pilot *et al.* 2006). Of particular interest is the suggestion of coupling of the heterochromatin assembly to a nuclear scaffold, which in turn connects it to the nuclear envelope (Nelson *et al.* 1986; Labrador & Corces 2002; Zhang *et al.* 2005). The highly compacted chromatin regions are organized along the nuclear periphery and are thought

*Author for correspondence (dbsgvs@nus.edu.sg).

One contribution to a Theme Supplement 'Mechanobiology'.

Received 29 January 2010
Accepted 8 March 2010

to be anchored to the lamin network at distinct foci (Dahl *et al.* 2005). This anchorage may be mediated by the interactions of HP1 (heterochromatin protein 1) with Lamin A and LBR (Lamin B receptor, which in turn interacts with the B type lamins) in the nuclear membrane (Makatsori *et al.* 2004; Gruenbaum *et al.* 2005). In addition, our previous work had suggested heterochromatin nodes to be an integral component of the structural organization of the cell nucleus (Mazumder & Shivashankar 2007). But experiments are few that mechanistically test whether heterochromatin acts as nodes of nuclear architecture. There has been a recent suggestion that the organization of the heterochromatin is thought to be connected to that of the nuclear lamina (Raz *et al.* 2006). A recent finding further establishes centromeric heterochromatin to be a primary load-bearer for microtubule-based forces governing nuclear morphology in fission yeast (King *et al.* 2008). Hence, in addition to the histone proteins, an elaborate network of non-histone proteins governs morphology of the cell nucleus, and its position inside the cell and attachment of the cytoskeleton to the nucleus (Patterson *et al.* 2004; Lee *et al.* 2007; Hale *et al.* 2008). Despite this, the possibility of prestress on the cell nucleus whereby it is held under a balance of opposing forces has not been fully elucidated.

In this work we studied the response of the cell nucleus to a number of physical and chemical stresses to investigate the structural maintenance of nuclear organization within living cells. The present work details the components of nuclear prestress, and traces its effects on processes of differentiation and development. To assess the relative contributions of the cytoskeletal systems on nuclear organization, we systematically measured nuclear size under chemical perturbations. Variations of nuclear size in primary mouse embryonic fibroblast (PMEF) cells indicate a compressive loading by microtubules and pulling forces owing to the actomyosin cytoskeleton. These forces act in addition to the intrinsic forces due to the entropic nature of the DNA polymer opposed by histone and other nuclear proteins (Mazumder *et al.* 2008). The net balance of such forces gives the cell nucleus its effective morphology. Laser ablations in combination with chemical perturbations established that the nucleus is held under tension by the actomyosin system. Next, we mapped the onset of nuclear prestress in differentiation and development. Previous work in the literature had shown that, in undifferentiated cells, nuclear components are plastic (Meshorer & Misteli 2006; Meshorer *et al.* 2006; Pajerowski *et al.* 2007). Here, we show that nuclear prestress due to the cytoskeleton is also largely absent in embryonic stem (ES) cells but develops with differentiation. A similar emergence of nuclear prestress is also demonstrated in the cellularization of the early *Drosophila* embryo. Thus, such organizing principles are not a peculiarity of nuclei in cells growing in monolayer cultures, but are more general and apply even to an organism. Across a variety of platforms nuclear prestress is established to be a mechanistic regulator of nuclear morphology.

2. MATERIAL AND METHODS

2.1. Cell culture and drug treatments

All cell culture products were from Gibco, Invitrogen, Carlsbad, CA, USA, unless otherwise mentioned. PMEF cells were cultured with DMEM-F12 supplemented with 5 per cent foetal bovine serum (FBS), penicillin–streptomycin. Cells were maintained at 37°C in a 5 per cent CO_2 incubator. PMEF cells up to third passage were used in experiments. R1 ES cells were cultured on a layer of feeder cells (PMEF) with DMEM-F12 supplemented with 15 per cent FBS (Hyclone, Logan, UT, USA), 1 mM sodium pyruvate, 0.1 mM non-essential amino acids, 2 mM L-glutamine, 0.1 mM β-mercaptoethanol, penicillin–streptomycin and 500 U ml^{-1} leukaemia inhibitory factor (LIF) (from Sigma–Aldrich, St Louis, MO, USA). Both cell types were cultured on glass-bottom coverslip dishes for transfection with Effectene transfection reagent (Qiagen, Valencia, CA, USA) according to the manufacturer's instructions. Cells were imaged 24 h later. For differentiation, ES cells were taken off feeders and plated onto coverslip dishes in the presence of LIF. After 1 day, LIF was withdrawn and cells were left to differentiate in LIF-free medium for 4 more days. Transfections were carried out in the differentiated cells as before. All results pertaining to PMEF in this work refer to these cells transfected with H1e–enhanced green fluorescent protein (EGFP), unless otherwise stated. H1e–EGFP-transfected PMEF cells were treated with the respective drugs 24 h post-transfection. The drug concentrations used were as follows: for depolymerizing microtubules, nocodazole: 1 μg ml^{-1}, 16 h; for depolymerizing actin, cytochalasin D: 1 μM, 2.5 h; for inhibiting myosin II, blebbistatin: 5 μM, 2.5 h (all drugs were procured from Sigma–Aldrich).

2.2. Drosophila *embryo collection*

For experiments using *Drosophila* embryos, a transgenic line in which one of the core histones, H2B, is tagged to EGFP (H2B–EGFP) was used. Flies were kept for 1 h on a sucrose–agar plate for egg laying. Collected embryos were washed and mounted on a no. 1 coverslip with the dorsal side facing downwards and covered with Halocarbon oil 700 (Sigma–Aldrich).

2.3. Imaging and ablations

Experiments were performed on a Zeiss LSM 510 Meta confocal microscope using a 40×, 1.3 N.A. objective (Carl Zeiss, Jena, Germany). Ablation experiments were performed using titanium–sapphire 80 MHz pulsed femtosecond lasers (Tsunami or Mai-Tai—Spectra Physics, Mountain View, CA, USA) mode-locked at 835 nm as described before (Mazumder & Shivashankar 2007). Subcellular perturbations of heterochromatin nodes or of the cell cytoplasm were carried out using an approximately 6.8 s scan of a 1.5 μm diameter region (approx. 75 mW at a fixed spot). The cells were then monitored for several minutes.

2.4. Image and statistical analyses

All quantification of fluorescence images captured on the confocal microscope was performed using LabVIEW (National Instruments, Austin, TX, USA), or Image J (public domain software developed at the National Institutes of Health, Bethesda, MD, USA). For calculating areas or volumes of nuclei, images were converted to binary-thresholded images. As explained before, nuclear area was used under conditions in which the z spans of the nuclei were similar. Alternatively, nuclear volumes were evaluated (e.g. for isolated nuclei or in the *Drosophila* embryo). The same thresholds were uniformly used for all sets of images of different perturbations in any one experiment. A Student's t-test was performed for all tests of significance, using Microcal Origin 6.0 (Originlab, Northampton, MA, USA). All graphs were also plotted using the Origin software.

3. RESULTS

3.1. Chemical disruption of cytoskeletal filaments alters nuclear morphology

Cellular prestress has been widely investigated in terms of cytoskeletal architecture (Ingber 2008; Wang *et al.* 2009), in which actin cytoskeleton has been implicated as the prime mediator of tension in cells (Padmakumar *et al.* 2005), whereas microtubules with their large persistence lengths apply compressive stresses (Elbaum *et al.* 1996). Based on this, we reasoned that chemical perturbations of such cytoplasmic components should affect nuclear size. PMEF cells were treated with various drugs, fixed, then DNA-stained with Hoechst dye and the nuclei were measured for the largest cross-sectional area from a collection of confocal images (figure 1*a*,*b*). Depolymerizing microtubules with nocodazole caused nuclei in cells to enlarge, while depolymerizing actin with cytochalasin D in contrast caused a drastic reduction in nuclear size. Motor proteins act in conjunction with filaments to apply stresses. When the major myosin isoform myosin II was inhibited with blebbistatin, interestingly, a significant reduction in nuclear size was observed, although nuclear shape was less perturbed than with actin depolymerization. With actin depolymerization, the nuclear size approaches that of isolated nuclei (figure 1*b*), when a nucleus has been taken out of the cytoplasmic milieu. Taken together, these chemical perturbations of the cytoskeleton indicate that the actomyosin complex provides an outward pull on the nucleus, while the microtubule cytoskeleton applies pushing forces. Such a distribution of forces conforms to models of cellular tensegrity, which also predicts a prestressed state of the cell nucleus (Ingber 1993, 2008). To rule out non-specific effects of these chemical inhibitors, we then tested the prestressed state of the nucleus with a direct physical perturbation using laser ablation.

3.2. Probing structural integrity of the cell nucleus using laser ablation

An earlier study had shown that laser perturbation of heterochromatin assembly, but not euchromatin,

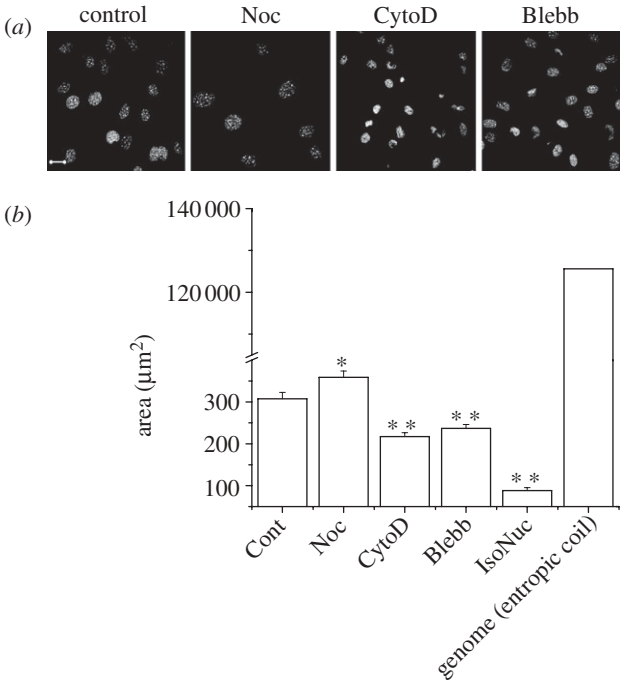

Figure 1. Chemical depolymerization of cytoplasmic filaments or inhibition of associated motor proteins cause a variation in nuclear size in PMEF cells. (*a*) Representative images of drug-treated and fixed nuclei with the DNA-stained with Hoechst dye. Scale bar, 20 μm. (*b*) Statistics for approximately 100 nuclei each. The error bars are standard errors. Cont, control; Noc, nocodazole; CytoD, cytochalasin D; Blebb, blebbistatin; IsoNuc, isolated nucleus. Also shown are the x–y projected area of nuclei isolated from PMEF cells ($n = 19$) and the estimated hydrodynamic radius of the genome in these cells. The error bars shown are standard deviations. Student's t-test: $^{*}p < 0.05$; $^{**}p < 0.001$.

caused a rapid nuclear collapse over approximately 100 s in HeLa cells, suggesting a mechanical release of nuclear prestress (Mazumder & Shivashankar 2007). Further, heterochromatin ablation was accompanied by disintegration of the actin and microtubule cytoskeletons but not of intermediate filaments. To probe the spatial architecture of nuclear prestress in PMEF cells, which are primary cells with sharp heterochromatin nodes, we used subcellular laser perturbations of heterochromatin nodes. Live PMEF cells expressing EGFP-tagged histone proteins (H1e–EGFP or H2B–EGFP) as chromatin markers were used in these studies. Cell shape and size did not change as drastically under conditions of nuclear shrinkage owing to heterochromatin ablation (figure 2*a*), although there were indicators of loss of membrane tension owing to the perturbed actin cytoskeleton. This indicates a decoupling of the nucleus from the residual cytoskeleton. The shrinkage in the x–y plane was accompanied by a slight expansion in the z plane. The net result was an approximately 33 per cent decrease in nuclear volume. A further proof for reduction in nuclear volume comes from the rise in the intensity of confocal slices with a reduction in nuclear area (figure 2*b*,*c*). However, a redistribution of material without condensation of nuclear volume will not result in a rise in mean pixel intensity of H2B–EGFP. Such a rise in our experiments thus

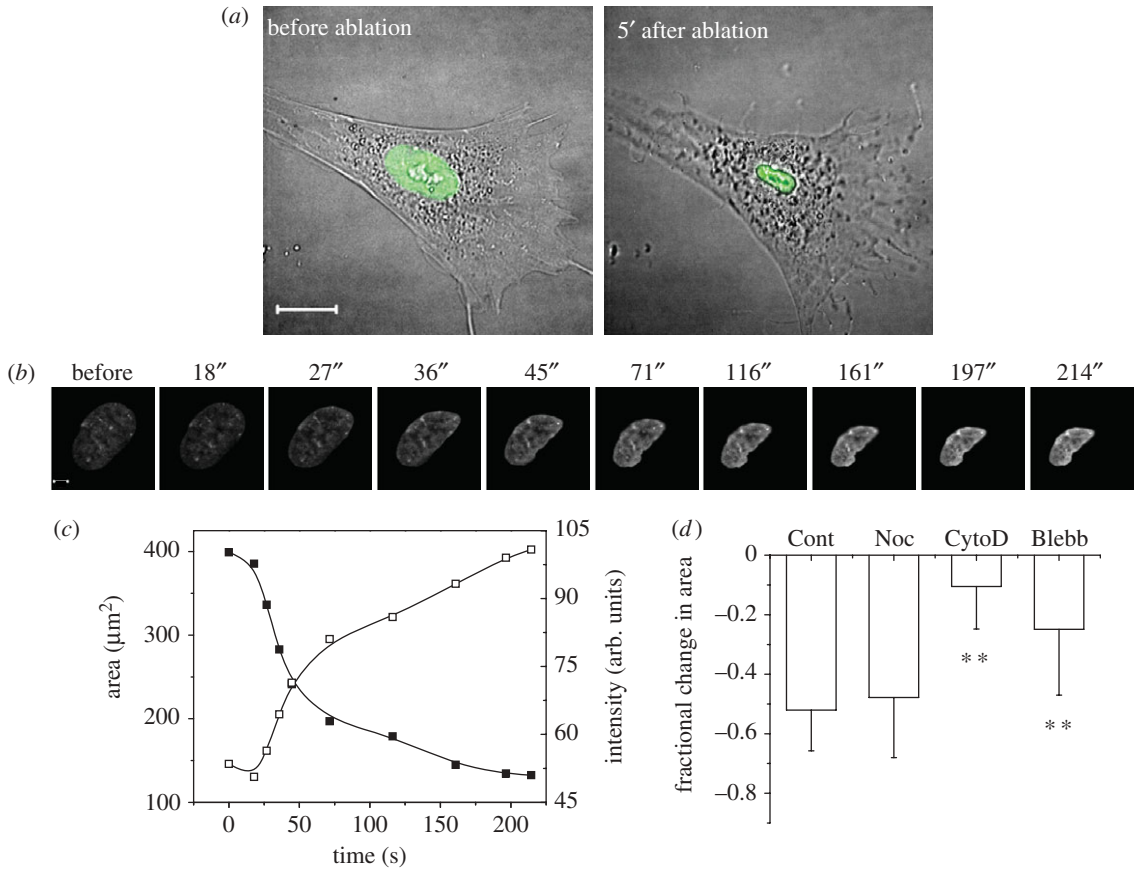

Figure 2. Effects of heterochromatin laser ablation on nuclear size. (*a*) The fluorescence image of the cell nucleus is super-imposed on differential interference contrast images of the cells. After ablation, cell shape does not change as much as the nucleus, although there are indications of a loss of membrane tension. Scale bar, 20 μm. (*b*) A further proof for reduction in nuclear volume comes from the rise in intensity of confocal slices with a reduction in nuclear area. We show it here for the shrinkage of a representative PMEF cell nucleus expressing histone H2B–EGFP as the chromatin marker. Images from every time point in the graph are presented in the panel above. Scale bar, 5 μm. (*c*) The fall in nuclear area is accompanied by a corresponding rise in mean pixel intensity in the area covered by the nucleus in (*b*). (*d*) Fractional change in area upon heterochromatin ablation for indicated drug treatments ($n = 15$, each). The error bars are standard deviations. Student's *t*-test, $^{**}p < 0.001$.

indicates a reduction in nuclear volume (hence, an increase in the density of a chromatin-bound protein). Since the shrinkage was most pronounced in the x–y direction for cells growing in monolayer cultures with a smaller increase in height in z, further experiments used reduction in nuclear area to quantify nuclear shrinkage.

Laser perturbation of heterochromatin nodes was then combined with chemical cytoplasmic perturbations in PMEF cells (figure 2*d*). The fractional change in area at the end of approximately 7 min for ablations under conditions of various cytoplasmic chemical perturbations was compared with untreated cells. Microtubules showed negligible effects on shrinkage dynamics. However, when myosin II was inhibited, and most markedly when actin was depolymerized, the fractional decrease in area was significantly less than that for control cells, suggesting that the outward tension had already been considerably relieved in these cells. These laser ablation studies of nuclear size thus confirmed that it is the actomyosin system which actively exerts an outward pull on the cell nucleus, as also suggested by previous studies (Sims *et al.* 1992).

3.3. Anisotropy in the distribution of prestress around an elliptical nucleus

In many experiments, ablation at the heterochromatin in PMEF cells resulted in an anisotropic shrinkage of the cell nucleus with a drastic reduction of the short axis, and marginal effects on the long axis (figure 3*a*). That the major contraction should occur along the short axis in response to heterochromatin ablation indicates an anisotropic distribution of nucleo-cytoplasmic contacts where the prime concentration of such anchors is likely to be at the ends of the elliptical nucleus. This was further confirmed by cytoplasmic ablations at these ends, which caused nuclear shrinkage with no increase in nuclear shape anisotropy (figure 3*a*–*c*). This was quantified by measuring the circularity of the nuclei, defined as $C = 4\pi \times \text{area}/\text{perimeter}^2$. $C = 1$ for a perfect circle, and decreases as the nuclei tend to become more elliptical. Thus heterochromatin ablation caused a large negative change in circularity, while cytoplasmic ablations left it predominantly unchanged. The large error bars indicate the heterogeneity in shape change responses. In cells with anisotropic nuclei, the long axis of the nucleus was oriented along the first principal

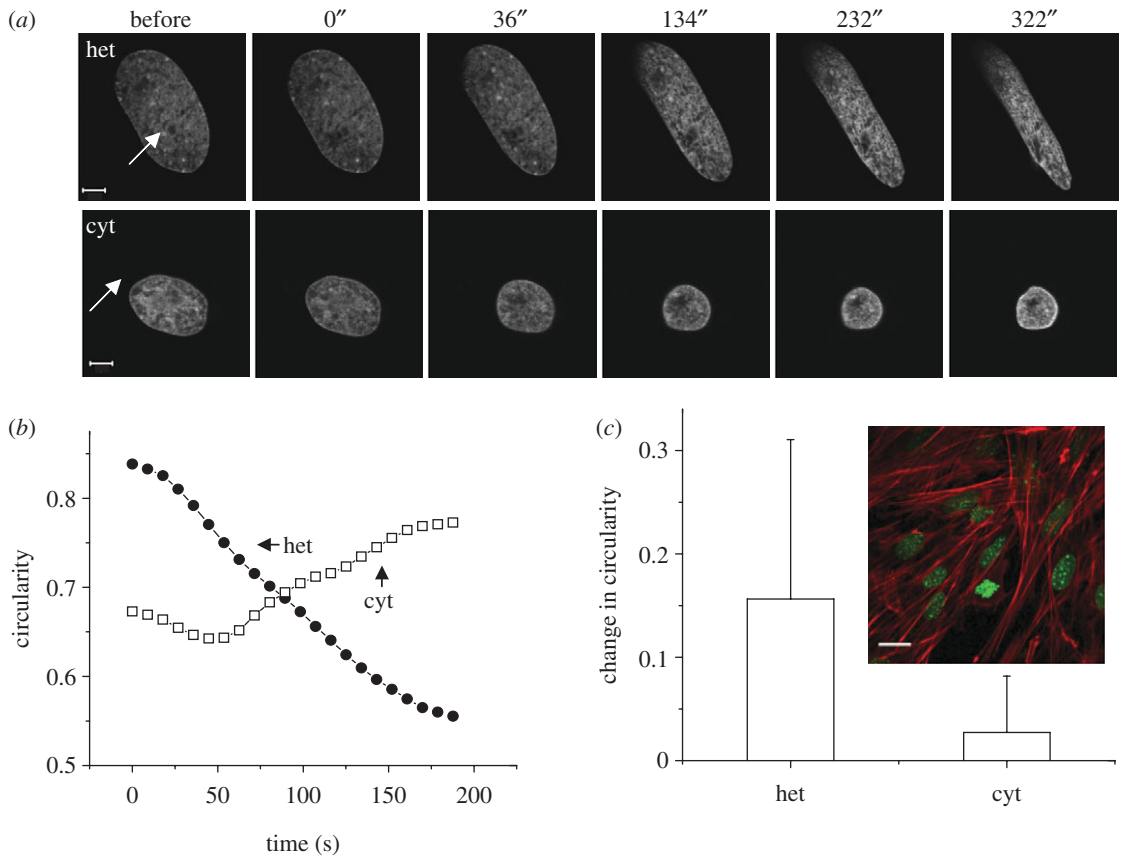

Figure 3. Effects of heterochromatin laser ablation on nuclear shape. (*a*) Shape changes upon heterochromatin (het) and cytoplasmic (cyt) ablations—representative images (time in seconds is indicated on top of the panel; scale bar, 5 μm), (*b*) representative time traces for change in circularity and (*c*) statistics of change in circularity ($n = 10$). Inset: elongated nuclei align along actin stress fibres (DNA was stained with Hoechst dye (1 μg ml^{-1}) (green) and actin with tetramethyl rhodamine isothiocyanate (TRITC)-phalloidin (1 μM) (red), cells fixed in 4% paraformaldehyde (PFA) and imaged). Scale bar, 20 μm. All error bars are standard deviations.

axis of the cell, i.e. in the direction of the actin stress fibres (figure 3*c*). Thus, the predominant direction of tension owing to the actomyosin complex is along the long axis of a cell nucleus in this cell type. Earlier experiments had also suggested a mechanical coupling of the nucleus to the cytoskeleton and such a non-uniform distribution of contacts around the envelope (Maniotis *et al.* 1997).

3.4. Mapping the role of cytoskeletal and nuclear filaments in maintaining nuclear prestress

Previous fixed and live cell studies showed a disruption of actin and microtubule cytoskeletons accompanying heterochromatin ablation and a collapse of the nucleus (Mazumder & Shivashankar 2007). In PMEF cells, direct laser ablation of the cytoplasmic elements resulted in nuclear shrinkage, and the effects were most pronounced when actin stress fibres were targeted (figure 4*a*,*b*). This further established the role of the actin filaments in applying tension on the cell nucleus.

The nucleoskeleton constituted from the type V intermediate filament lamins and other proteins mediates contacts between the cytoskeleton and the nuclear interior. In PMEF cells cotransfected with EGFP–Lamin B1 and H1e–monomeric red fluorescent protein (mRFP), the nuclear lamina exhibited indentations parallel to the long axis (figure 4*c*). Our earlier work in HeLa cells had shown that the nuclear lamina as marked by EGFP–Lamin B1 undergoes a concomitant shrinkage with nuclear collapse upon heterochromatin ablation (Mazumder & Shivashankar 2007). Indeed, an siRNA-mediated knockdown of lamin B1 in such HeLa cells produces a marginal reduction in the shrinkage response (figure 4*d*). As discussed before, a number of studies have suggested the coupling of dense nodes of chromatin to the nuclear lamins (Labrador & Corces 2002; Makatsori *et al.* 2004; Dahl *et al.* 2005; Gruenbaum *et al.* 2005; Raz *et al.* 2006). Thus, it is perhaps a coupling of the chromatin and the lamin scaffold which makes heterochromatin assemblies such vital nodes of nuclear architecture.

3.5. Emergence of nuclear prestress in cellular differentiation

Next, we mapped the onset of nuclear prestress in processes of cellular differentiation and development. Previous observation has shown that the nuclear architecture in human ES cells is highly plastic, where micropipette aspiration experiments revealed a sixfold rise in nuclear stiffness with differentiation (Pajerowski *et al.* 2007). Recent work also suggests that the softer

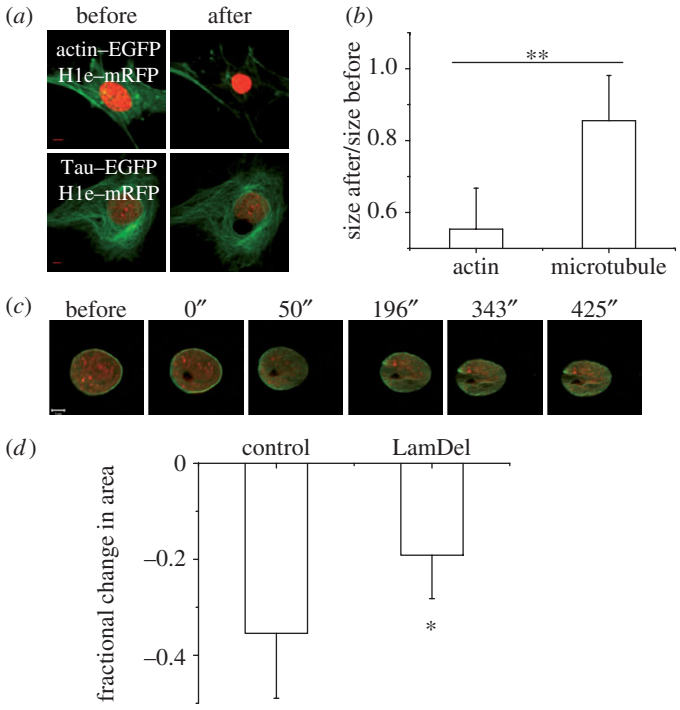

Figure 4. Effects of laser ablation on structural filaments. (*a*) PMEF cells were cotransfected with H1e–mRFP and either one of actin–EGFP or Tau–EGFP. Forty-eight hours post-transfection ablation experiments were performed (80 mW, 3.4 s) to sever actin stress fibres or microtubules locally. Images of representative cells reconstructed by *z* projection from confocal stacks are shown. Note the large shrinkage in nuclear size when actin is perturbed. (*b*) Ratio of the largest cross-sectional areas after and before ablation are plotted for perturbation of the actin and microtubule cytoskeletons ($n = 8$ and 6). The relative shrinkage is greater for perturbation of the actin stress fibres. (*c*) EGFP–Lamin B1 and H1e–mRFP cotransfected PMEF cells were ablated at the heterochromatin. Time course in a merged image is presented. Note the indentations in the lamin scaffold. The time points are indicated above the panel. Scale bar, 5 μm. (*d*) HeLa cells expressing H2B–EGFP were cotransfected with an siRNA against Lamin B1, and a plasmid-expressing mRFP. Forty-eight hours post-transfection, such cells showed a lesser response to heterochromatin ablation (120 mW, 3.4 s) than control cells transfected just with the mRFP plasmid ($n = 8$ each). mRFP-expressing cells were considered in both cases to identify transfected cells. The error bars shown are standard deviations. Student's *t*-test: $^{*}p < 0.05$; $^{**}p < 0.001$. The error bars are standard deviations.

ES cells are more sensitive to forces than differentiated cells (Chowdhury *et al.* 2010). Thus, nuclear prestress could possibly emerge during cellular differentiation. In addition, previous studies have suggested a plastic state of the chromatin in terms of enhanced histone dynamics, and larger fluctuations of the nuclear envelope in undifferentiated murine R1 ES cells (Meshorer & Misteli 2006; Bhattacharya *et al.* 2009).

Hence, we further explored nuclear volumes in nuclei isolated from different cell types, to gain further insight with regards to prestress in a cellular context, as suggested in figure 1*b*. Reversible swelling of isolated nuclei under conditions of low salt has been demonstrated before (Dahl *et al.* 2005; Mazumder *et al.* 2008). Nuclei were isolated from murine R1 ES cells and PMEF cells according to methods described previously (Mazumder *et al.* 2008). The isolated nuclei were mounted on poly-D-lysine-coated coverslips, stained with Hoechst 33342 and imaged in phosphate-buffered saline (PBS). When PBS is replaced with water, the nuclei undergo a swelling in size. The process is reversible and, once the salt conditions are brought back to those of a physiological buffer PBS, the initial configurations of the nuclei are restored with a high fidelity. We quantified the nuclear volume under these conditions, and compared it with that inside cells (figure 5*a*). Interestingly, nuclei isolated from PMEF cells showed a significant decrease in volume upon isolation, unlike ES cell nuclei. However, once the nuclei are isolated, nuclear volumes in PBS are comparable for both cell types, indicating that this is primarily governed by the genome size and nuclear architecture. As would then be expected, nuclei from both of these cell types show similar levels of swelling under conditions of low salt. The water-swollen limit probably indicates the maximum extent to which these nuclei can be stretched. Note that, in a cellular context, PMEF nuclei are indeed stretched nearly to this level but not so for ES nuclei. This provides an indication of a difference in nuclear prestress in a cytoplasmic context in PMEF cells as opposed to undifferentiated ES cells, which we confirmed by heterochromatin ablation experiments. With differentiation of R1 ES cells, nuclear morphology starts to resemble terminally differentiated primary cells such as PMEF cells in having a smoother nuclear contour and distinct heterochromatin foci (figure 5*b*). Heterochromatin ablation was carried out in ES cells and under conditions of differentiation, both transfected with H2B–EGFP. ES cells exhibit marginal nuclear collapse, while the differentiated cells respond similarly to PMEF cells upon ablation (figure 5*b*,*c*), suggesting a fluidic state of nuclear prestress in ES cells. A lower nuclear prestress in the undifferentiated stage, as

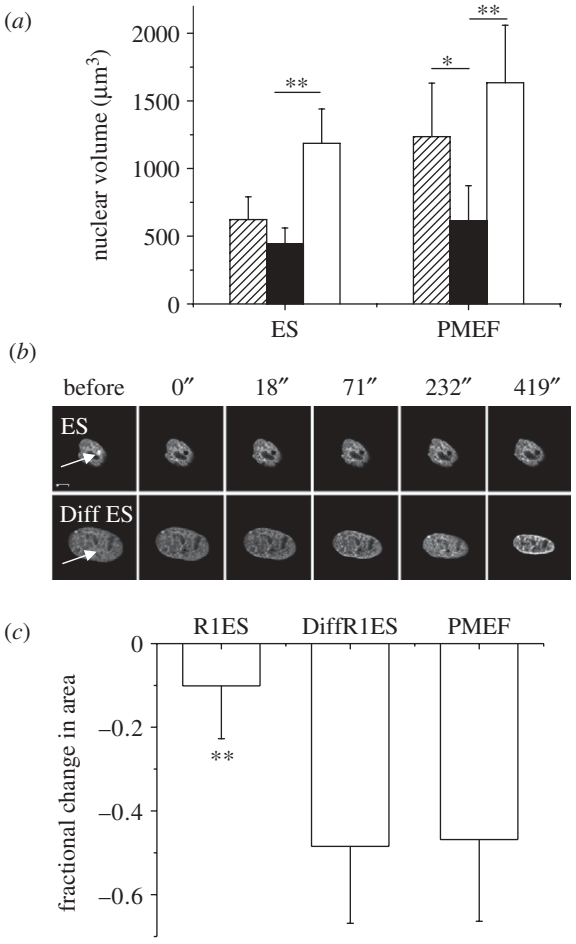

Figure 5. Emergence of nuclear prestress in differentiation. (*a*) Isolated nuclei from both R1 ES cells and PMEF cells show reversible swelling under conditions of low salt. Nuclear volumes are plotted for nuclei inside ES or PMEF cells (hatched bars), or nuclei isolated from such cells in PBS (black bars) or the same nuclei in water (open bars) ($n = 7$ each). Note that the relative size of the nucleus is larger in a cellular context for PMEF cells, while the level of water-induced swelling is similar and probably represents an upper bound for nuclear swelling. (*b*) Representative images of R1 ES cells and differentiated R1 ES cells upon heterochromatin ablation. Time in seconds is indicated on top of the panel. Scale bar, 5 μm. (*c*) Fractional change in area upon heterochromatin ablation for indicated cell types ($n = 17$ each). Student's *t*-test: $^{*}p < 0.05$; $^{**}p < 0.001$. The error bars are standard deviations.

indicated in figure 5*a*, is confirmed by these experiments. With cellular differentiation along with the stiffening of the nucleus, there is a concomitant emergence of nuclear prestress.

3.6. Emergence of nuclear prestress in the context of development

The architecture of a prestressed nucleus emerging from our study of cells in culture was then extended to a three-dimensional organismal context, where cell–cell contacts become important. During *Drosophila* embryogenesis, nuclei migrate to the periphery of the embryo at the eighth mitotic cycle, and, in the hour after the thirteenth mitotic cycle, cellularization of the blastoderm occurs. Notably, all the nuclei are spherical at interphase in the precellular blastoderm. Asymmetric nuclear shapes emerge upon cellularization, and some of the molecules in nuclear morphogenesis have been identified (Brandt *et al.* 2006; Pilot *et al.* 2006). The evolution of the signatures of nuclear prestress was monitored in a transgenic fly constitutively expressing histone H2B tagged to EGFP (Bhattacharya *et al.* 2006, 2009). In the early *Drosophila* embryo, the decrease in circularity in nuclear shape with the progression of cellularization indicated the onset of prestress, and highly anisotropic nuclear shapes emerged with germ band extension (figure 6*a*). Ablation experiments were then carried out in two distinct developmental stages of the embryo: one just before cellularization and the other after the onset of germ band extension. In the former, ablation resulted in mitotic defects (data not shown), and absence of nuclear prestress in the precellular embryo. In striking contrast, cytoplasmic or heterochromatin perturbations in the anisotropic nuclei of the germ band and amnioserosa cells caused a dramatic nuclear collapse (figure 6*b*,*c*). Thus, this indicates that the conditions of nuclear architectural integrity emerging from these studies are not a peculiarity of cells growing on monolayer cultures, but are true even in the context of a local three-dimensional microenvironment within an organism.

4. CONCLUSIONS

The present work investigates nuclear prestress by analysis of nuclear size under different physical and chemical stresses. An outward pull on the nuclear envelope, because of the actomyosin system and compressive loading by microtubules, was identified by measuring the size of nuclei in PMEF cells under conditions of chemical perturbations of such cytoskeletons. Our previous studies had shown the heterochromatin nodes to be vital load-bearing elements in maintaining nuclear structure (Mazumder & Shivashankar 2007). A recent finding further established the link between the cytoplasm and the nucleus, and suggests centromeric heterochromatin to be a primary load-bearer for microtubule-based forces governing nuclear morphology in fission yeast (King *et al.* 2008). The tension force on the nucleus was further verified in laser ablation studies, where heterochromatin ablation causes a nuclear collapse with actual condensation of nuclear volume. Both actin and microtubule cytoskeletons were affected during this process; however, cell shape was not as affected as nuclear morphology, indicating a decoupling of the nucleus from the cytoskeleton. In many instances, PMEF nuclei underwent anisotropic collapses, indicating that the nucleo-cytoplasmic contacts are not uniformly distributed around the nuclear envelope. As would be expected cytoplasmic ablations did not cause such anisotropic collapses.

We then mapped the onset of nuclear prestress in processes of cellular differentiation. Previous studies had reported a plastic state of nuclei in undifferentiated ES cells in terms of enhanced nuclear protein dynamics

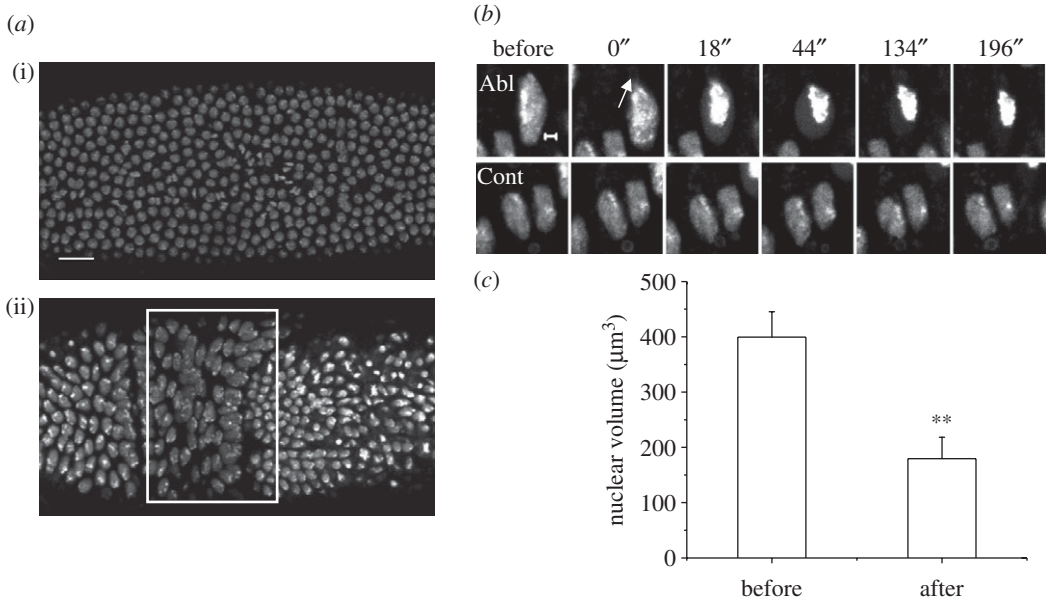

Figure 6. (*a*) Two distinct time points during *Drosophila* gastrulation—just after the 13th mitotic cycle (i) and after the onset of gastrulation (ii). The embryo is viewed from the dorsal side with the anterior to the left. The white rectangle indicates the nuclei of the germ band and amnioserosa cells. Scale bar, 20 μm. (*b*) Elongated cells of the germ band and early amnioserosa were ablated at the point indicated by the white arrow in the cytoplasm. Circularization and chromatin condensation were evident in the ablated cell, but not in control cells in the same neighbourhood. Scale bar, 2 μm. (*c*) The fall in nuclear volume is shown in the graph, before and after such ablations ($n = 5$). All error bars are standard deviations. Student's *t*-test, $^{**}p < 0.001$.

(Meshorer *et al.* 2006) and lesser nuclear stiffness (Pajerowski *et al.* 2007). Work from our own laboratory had shown a more fluidic state of the lamin scaffold in such cells (Bhattacharya *et al.* 2009). In good conformation with these studies, signatures of nuclear prestress again were lower in such cells. We further mapped the onset of nuclear prestress in a developing *Drosophila* embryo, thus showing the principles of nuclear organization emerging from our studies to be generally applicable even to the context of an organism. The nuclei in the early syncytial blastoderm were uniform in size and largely spherical, but a wide range of nuclear shapes emerged with cellularization of the embryo. Cytoplasmic ablations in highly anisotropic nuclei in this system also led to nuclear collapse. Mechanical stresses are found to alter cellular differentiation in culture (Engler *et al.* 2006), and developmental programmes in organisms (Farge 2003). Thus, the absence of prestress in undifferentiated cells, as found in our studies, could provide a flexible nuclear architecture poised for differentiation programmes.

In summary, the present study uses subcellular laser perturbations to further elucidate the structural organization of the eukaryotic nucleus. We show that the connections between nuclear and cytoplasmic elements are not passive, but actually serve to govern nuclear shape and size, and thus can be exploited by cells as a handle to fine-tune gene expression within the three-dimensional architecture of the nucleus. Emerging evidence indicates that spatio-temporal organization of chromatin and hence gene position is one of the regulators of gene expression programmes. Mechanical cues are known to alter gene transcription (Thomas *et al.* 2002; Dahl *et al.* 2008), cellular differentiation in culture (Engler *et al.* 2006) and developmental programmes in organisms (Farge 2003), suggesting a strong link between cellular architecture and information control within living cells. Thus, to address almost any nuclear function it becomes essential to elucidate the physical nature of the forces that maintain the eukaryotic nucleus. An interesting possibility that we are currently investigating is to verify whether nuclear prestress, as described in this work, may provide a substrate for organization of the genome, and thus of gene expression.

We thank the Nanoscience Initiative of the Department of Science and Technology for funding and the NCBS Common Imaging and Flow Facility supported in part by the Wellcome Trust. We thank Albert Libchaber (Rockefeller University) for very useful discussions and critical reading of the manuscript. Mouse R1 ES cells were a kind gift from Dr Maneesha Inamdar (JNCASR, India).

REFERENCES

Bhattacharya, D., Mazumder, A., Miriam, S. A. & Shivashankar, G. V. 2006 EGFP-tagged core and linker histones diffuse via distinct mechanisms within living cells. *Biophys. J.* **91**, 2326–2336. (doi:10.1529/biophysj.105.079343)

Bhattacharya, D., Talwar, S., Mazumder, A. & Shivashankar, G. V. 2009 Spatio-temporal plasticity in chromatin organization in mouse cell differentiation and during *Drosophila* embryogenesis. *Biophys. J.* **96**, 3832–3839. (doi:10.1016/j.bpj.2008.11.075)

Brandt, A. *et al.* 2006 Developmental control of nuclear size and shape by Kugelkern and Kurzkern. *Curr. Biol.* **16**, 543–552. (doi:10.1016/j.cub.2006.01.051)

Chowdhury, F., Na, S., Li, D., Poh, Y. C., Tanaka, T. S., Wang, F. & Wang, N. 2010 Material properties of the cell dictate stress-induced spreading and differentiation in embryonic stem cells. *Nat. Mater.* **9**, 82–88. (doi:10.1038/nmat2563)

Constantinescu, D., Gray, H. L., Sammak, P. J., Schatten, G. P. & Csoka, A. B. 2006 Lamin A/C expression is a marker of mouse and human embryonic stem cell differentiation. *Stem Cells* **24**, 177–185. (doi:10.1634/stemcells.2004-0159)

Crisp, M., Liu, Q., Roux, K., Rattner, J. B., Shanahan, C., Burke, B., Stahl, P. D. & Hodzic, D. 2006 Coupling of the nucleus and cytoplasm: role of the LINC complex. *J. Cell. Biol.* **172**, 41–53. (doi:10.1083/jcb.200509124)

Dahl, K. N., Engler, A. J., Pajerowski, J. D. & Discher, D. E. 2005 Power-law rheology of isolated nuclei with deformation mapping of nuclear substructures. *Biophys. J.* **89**, 2855–2864. (doi:10.1529/biophysj.105.062554)

Dahl, K. N., Ribeiro, A. J. & Lammerding, J. 2008 Nuclear shape, mechanics, and mechanotransduction. *Circ. Res.* **102**, 1307–1318. (doi:10.1161/CIRCRESAHA.108.173989)

Elbaum, M., Fygenson, D. K. & Libchaber, A. 1996 Buckling microtubules in vesicles. *Phys. Rev. Lett.* **76**, 4078–4081. (doi:10.1103/PhysRevLett.76.4078)

Engler, A. J., Sen, S., Sweeney, H. L. & Discher, D. E. 2006 Matrix elasticity directs stem cell lineage specification. *Cell* **126**, 677–689. (doi:10.1016/j.cell.2006.06.044)

Farge, E. 2003 Mechanical induction of Twist in the *Drosophila* foregut/stomodeal primordium. *Curr. Biol.* **13**, 1365–1377. (doi:10.1016/S0960-9822(03)00576-1)

Gruenbaum, Y., Margalit, A., Goldman, R. D., Shumaker, D. K. & Wilson, K. L. 2005 The nuclear lamina comes of age. *Nat. Rev. Mol. Cell. Biol.* **6**, 21–31. (doi:10.1038/nrm1550)

Hale, C. M., Shrestha, A. L., Khatau, S. B., Stewart-Hutchinson, P. J., Hernandez, L., Stewart, C. L., Hodzic, D. & Wirtz, D. 2008 Dysfunctional connections between the nucleus and the actin and microtubule networks in laminopathic models. *Biophys. J.* **95**, 5462–5475. (doi:10.1529/biophysj.108.139428)

Haque, F., Lloyd, D. J., Smallwood, D. T., Dent, C. L., Shanahan, C. M., Fry, A. M., Trembath, R. C. & Shackleton, S. 2006 SUN1 interacts with nuclear lamin A and cytoplasmic nesprins to provide a physical connection between the nuclear lamina and the cytoskeleton. *Mol. Cell. Biol.* **26**, 3738–3751. (doi:10.1128/MCB.26.10.3738-3751.2006)

Houben, F., Ramaekers, F. C., Snoeckx, L. H. & Broers, J. L. 2007 Role of nuclear lamina-cytoskeleton interactions in the maintenance of cellular strength. *Biochim. Biophys. Acta.* **1773**, 675–686. (doi:10.1016/j.bbamcr.2006.09.018)

Ingber, D. E. 1993 Cellular tensegrity: defining new rules of biological design that govern the cytoskeleton. *J. Cell Sci.* **104**, 613–627.

Ingber, D. E. 2008 Tensegrity-based mechanosensing from macro to micro. *Prog. Biophys. Mol. Biol.* **97**, 163–179. (doi:10.1016/j.pbiomolbio.2008.02.005)

King, M. C., Drivas, T. G. & Blobel, G. 2008 A network of nuclear envelope membrane proteins linking centromeres to microtubules. *Cell* **134**, 427–438. (doi:10.1016/j.cell.2008.06.022)

Kracklauer, M. P., Banks, S. M., Xie, X., Wu, Y. & Fischer, J. A. 2007 *Drosophila* klaroid encodes a SUN domain protein required for Klarsicht localization to the nuclear envelope and nuclear migration in the eye. *Fly* (*Austin*) **1**, 75–85.

Labrador, M. & Corces, V. G. 2002 Setting the boundaries of chromatin domains and nuclear organization. *Cell* **111**, 151–154. (doi:10.1016/S0092-8674(02)01004-8)

Lammerding, J., Fong, L. G., Ji, J. Y., Reue, K., Stewart, C. L., Young, S. G. & Lee, R. T. 2006 Lamins A and C but not lamin B1 regulate nuclear mechanics. *J. Biol. Chem.* **281**, 25 768–25 780. (doi:10.1074/jbc.M513511200)

Lanctot, C., Cheutin, T., Cremer, M., Cavalli, G. & Cremer, T. 2007 Dynamic genome architecture in the nuclear space: regulation of gene expression in three dimensions. *Nat. Rev. Genet.* **8**, 104–115. (doi:10.1038/nrg2041)

Lee, J. S., Hale, C. M., Panorchan, P., Khatau, S. B., George, J. P., Tseng, Y., Stewart, C. L., Hodzic, D. & Wirtz, D. 2007 Nuclear lamin A/C deficiency induces defects in cell mechanics, polarization, and migration. *Biophys. J.* **93**, 2542–2552. (doi:10.1529/biophysj.106.102426)

Makatsori, D., Kourmouli, N., Polioudaki, H., Shultz, L. D., McLean, K., Theodoropoulos, P. A., Singh, P. B. & Georgatos, S. D. 2004 The inner nuclear membrane protein lamin B receptor forms distinct microdomains and links epigenetically marked chromatin to the nuclear envelope. *J. Biol. Chem.* **279**, 25 567–25 573. (doi:10.1074/jbc.M313606200)

Maniotis, A. J., Chen, C. S. & Ingber, D. E. 1997 Demonstration of mechanical connections between integrins, cytoskeletal filaments, and nucleoplasm that stabilize nuclear structure. *Proc. Natl Acad. Sci. USA* **94**, 849–854. (doi:10.1073/pnas.94.3.849)

Mazumder, A. & Shivashankar, G. V. 2007 Gold-nanoparticle-assisted laser perturbation of chromatin assembly reveals unusual aspects of nuclear architecture within living cells. *Biophys. J.* **93**, 2209–2216. (doi:10.1529/biophysj.106.102202)

Mazumder, A., Roopa, T., Basu, A., Mahadevan, L. & Shivashankar, G. V. 2008 Dynamics of chromatin decondensation reveals the structural integrity of a mechanically prestressed nucleus. *Biophys. J.* **95**, 3028–3035. (doi:10.1529/biophysj.108.132274)

Meshorer, E. & Misteli, T. 2006 Chromatin in pluripotent embryonic stem cells and differentiation. *Nat. Rev. Mol. Cell. Biol.* **7**, 540–546. (doi:10.1038/nrm1938)

Meshorer, E., Yellajoshula, D., George, E., Scambler, P. J., Brown, D. T. & Misteli, T. 2006 Hyperdynamic plasticity of chromatin proteins in pluripotent embryonic stem cells. *Dev. Cell* **10**, 105–116. (doi:10.1016/j.devcel.2005.10.017)

Misteli, T. 2007 Beyond the sequence: cellular organization of genome function. *Cell* **128**, 787–800. (doi:10.1016/j.cell.2007.01.028)

Nelson, W. G., Pienta, K. J., Barrack, E. R. & Coffey, D. S. 1986 The role of the nuclear matrix in the organization and function of DNA. *Annu. Rev. Biophys. Biophys. Chem.* **15**, 457–475. (doi:10.1146/annurev.bb.15.060186.002325)

Padmakumar, V. C., Libotte, T., Lu, W., Zaim, H., Abraham, S., Noegel, A. A., Gotzmann, J., Foisner, R. & Karakesisoglou, I. 2005 The inner nuclear membrane protein Sun1 mediates the anchorage of Nesprin-2 to the nuclear envelope. *J. Cell Sci.* **118**, 3419–3430. (doi:10.1242/jcs.02471)

Pajerowski, J. D., Dahl, K. N., Zhong, F. L., Sammak, P. J. & Discher, D. E. 2007 Physical plasticity of the nucleus in stem cell differentiation. *Proc. Natl Acad. Sci. USA* **104**, 15 619–15 624. (doi:10.1073/pnas.0702576104)

Patterson, K., Molofsky, A. B., Robinson, C., Acosta, S., Cater, C. & Fischer, J. A. 2004 The functions of Klarsicht and nuclear lamin in developmentally regulated nuclear migrations of photoreceptor cells in the *Drosophila* eye. *Mol. Biol. Cell.* **15**, 600–610. (doi:10.1091/mbc.E03-06-0374)

Pilot, F., Philippe, J. M., Lemmers, C., Chauvin, J. P. & Lecuit, T. 2006 Developmental control of nuclear

morphogenesis and anchoring by charleston, identified in a functional genomic screen of *Drosophila* cellularisation. *Development* **133**, 711–723. (doi:10.1242/dev.02251)

Raz, V. *et al.* 2006 Changes in lamina structure are followed by spatial reorganization of heterochromatic regions in caspase-8-activated human mesenchymal stem cells. *J. Cell Sci.* **119**, 4247–4256. (doi:10.1242/jcs.03180)

Riemer, D., Stuurman, N., Berrios, M., Hunter, C., Fisher, P. A. & Weber, K. 1995 Expression of *Drosophila* lamin C is developmentally regulated: analogies with vertebrate A-type lamins. *J. Cell Sci.* **108**, 3189–3198.

Roux, K. J., Crisp, M. L., Liu, Q., Kim, D., Kozlov, S., Stewart, C. L. & Burke, B. 2009 Nesprin 4 is an outer nuclear membrane protein that can induce kinesin-mediated cell polarization. *Proc. Natl Acad. Sci. USA* **106**, 2194–2199. (doi:10.1073/pnas.0808602106)

Schermelleh, L. *et al.* 2008 Subdiffraction multicolor imaging of the nuclear periphery with 3D structured illumination microscopy. *Science* **320**, 1332–1336. (doi:10.1126/science.1156947)

Sims, J. R., Karp, S. & Ingber, D. E. 1992 Altering the cellular mechanical force balance results in integrated changes in cell, cytoskeletal and nuclear shape. *J. Cell Sci.* **103**, 1215–1222.

Stewart, C. L., Roux, K. J. & Burke, B. 2007 Blurring the boundary: the nuclear envelope extends its reach. *Science* **318**, 1408–1412. (doi:10.1126/science.1142034)

Thomas, C. H., Collier, J. H., Sfeir, C. S. & Healy, K. E. 2002 Engineering gene expression and protein synthesis by modulation of nuclear shape. *Proc. Natl Acad. Sci. USA* **99**, 1972–1977. (doi:10.1073/pnas.032668799)

Tzur, Y. B., Wilson, K. L. & Gruenbaum, Y. 2006 SUN-domain proteins: 'Velcro' that links the nucleoskeleton to the cytoskeleton. *Nat. Rev. Mol. Cell. Biol.* **7**, 782–788. (doi:10.1038/nrm2003)

Vergnes, L., Peterfy, M., Bergo, M. O., Young, S. G. & Reue, K. 2004 Lamin B1 is required for mouse development and nuclear integrity. *Proc. Natl Acad. Sci. USA* **101**, 10 428–10 433. (doi:10.1073/pnas.0401424101)

Wang, N., Tytell, J. D. & Ingber, D. E. 2009 Mechanotransduction at a distance: mechanically coupling the extracellular matrix with the nucleus. *Nat. Rev. Mol. Cell. Biol.* **10**, 75–82. (doi:10.1038/nrm2594)

Zhang, Q., Ragnauth, C. D., Skepper, J. N., Worth, N. F., Warren, D. T., Roberts, R. G., Weissberg, P. L., Ellis, J. A. & Shanahan, C. M. 2005 Nesprin-2 is a multi-isomeric protein that binds lamin and emerin at the nuclear envelope and forms a subcellular network in skeletal muscle. *J. Cell Sci.* **118**, 673–687. (doi:10.1242/jcs.01642)